International Journal of Thermophysics, Vol. 17, No. 3, 1996

Critical Dynamics in Microgravity[1]

R. Duncan,[2,3] S. Boyd,[2] W. Moeur,[4] S. Robinson,[3] R. Akau,[2] and S. Gianoulakis[2]

Although many well-controlled experiments have been conducted to measure the static properties of systems near criticality, few experiments have explored the transport properties in systems driven very far away from equilibrium as the transition occurs. Here we propose to measure the thermal gradient across the superfluid (HeII)—normal fluid (HeI) interface in microgravity conditions as a function of the heat flux Q used to make the measurements. Microgravity conditions are required (1) to avoid the hydrostatic pressure variation along the height of the helium column (a concern for $Q < 0.1\,\mu W \cdot cm^{-2}$), (2) avoid convection in He-I for $Q > 3\,\mu W \cdot cm^{-2}$ in our apparatus, and (3) to increase the $Q = 0$ interfacial width from its value of a few tens of microns on Earth to about a millimeter in orbit. New technologies described in this paper are under development for this experiment, which is in definition for Space Shuttle flight.

KEY WORDS: microgravity; critical phenomena; nonequilibrium; transport properties; thermal conductivity; low temperatures; superfluid helium; thermometry; superconducting instrumentation.

1. INTRODUCTION

The superfluid transition in pure liquid ^{4}He provides an excellent opportunity to test modern theories of second-order phase transitions. The ^{4}He sample is ultrapure, with only the ^{3}He isotope presenting an impurity. Typically this ^{3}He impurity level can be reduced to a part in 10^9 [1], and impurity levels as low as a few parts in 10^{12} have been reported [2]. Unlike

[1] Paper presented at the Twelfth Symposium on Thermophysical Properties, June 19–24, 1994, Boulder, Colorado, U.S.A.

[2] Sandia National Laboratories, Albuquerque, New Mexico 87185, U.S.A.

[3] University of New Mexico, Albuquerque, New Mexico 87131, U.S.A.

[4] To whom correspondence should be addressed.

0195-928X/96/0500-0631$09.50/0

solid samples, which support vacancies and grain boundaries even in the high-purity limit, the ^{4}He near its superfluid transition is homogeneous.

The order parameter in superfluid ^{4}He has two components, and it is often referred to as the "wavefunction of the condensate," consistent with the psi theory of superfluidity [3]. In most critical-phenomena studies, the field conjugate to the order parameter creates a rounding of the transition. The ^{4}He superfluid transition is unusual in that this field is not physical [3], and hence the superfluid transition in ^{4}He remains sharp. Since the superfluid transition temperature varies with pressure ($-113\,\text{bar}\cdot\text{K}^{-1}$ near saturated vapor pressure (SVP) [4]), the superfluid transition varies with the hydrostatic pressure along the height of the ^{4}He column under Earth's gravity. To avoid these gravitational-induced sample pressure gradients, extremely precise heat capacity measurements in bulk ^{4}He have been conducted in Earth orbit in late 1992 [5]. Another heat capacity experiment, one in a confined geometry where finite-size effects are measurable, is now under development for space deployment in 1997 [6].

Although static critical phenomena are relatively well studied, very little is known about transport properties through criticality in general. This is unfortunate, since in nature virtually all phase transitions occur while being driven far away from equilibrium conditions. Hence a first-principles understanding of critical phenomena under highly nonequilibrium conditions is of fundamental importance to virtually all real-world processes. In transport measurements the system is held out of equilibrium and maintained in an exceptionally well-controlled steady-state condition. In these experiments, the thermal gradients very near the normal fluid–superfluid interface (HeI–HeII) are then measured with sub-nanokelvin-resolved thermometry [7]. Under gravity the position of the HeI–HeII interface may be set (or maintained) by adjusting (or regulating) the temperature of the superfluid component. This superfluid component is isothermal in the low-heat flux (Q) limit, which is realized in our experiments. In Earth orbit this interface should be stabilized by the heat flux as predicted by theory [8], however these experiments do not depend upon this predicted stabilization in order to obtain the data once in Earth orbit.

2. SCIENTIFIC MOTIVATION

Recently, dynamic renormalization group theory (DRGT) has been applied to predict the thermal profile through the HeI–HeII interface subjected to a heat flux Q [9]. This theory predicts that the effective thermal conductivity of the HeI does not diverge but, rather, approaches a constant value which itself is strongly dependent on Q, as $T \to T_\lambda$. If this prediction is realized experimentally, it will constitute the first study of how a system's

linear response to an external heat flux breaks down near criticality, resulting in a nonohmic thermal conductivity. This theory [9], and another theory based primarily on a dynamic scaling approach [8], predicts that the width of the HeI–HeII interface will decrease with increasing heat flux as $1/\sqrt{Q}$. Since this interfacial width is essentially the correlation length at the superfluid transition temperature T_λ [$\xi(T=T_\lambda)$], these measurements would provide us with the first measurement of how the correlation length in a system at criticality varies with the nonequilibrium parameter (in our case the heat flux Q).

Both the renormalization group theory [9, 10] and the dynamic scaling theory [8] have predicted a depression of the superfluid transition temperature T_λ by the heat flux Q. This effect has been observed experimentally [11], and only small discrepancies exist between the theory [10] and the experimental result. For small Q, the helium is isothermal below $T_\lambda(Q)$ [11]. The nature of the thermal profile within the helium at temperatures $T_\lambda(Q) < T < T_\lambda(Q=0)$ is as yet unknown. Its determination remains an exciting challenge.

Measurements of the bulk helium properties described above are plagued by the presence of the experiment cell's end plates, especially very close to the superfluid transition temperature, where these boundary effects diverge. The thermal resistance between superfluid helium and a solid (usually metal) end plate, which is referred to as the Kapitza resistance, has been observed to be weakly singular at T_λ and to exhibit a sudden onset to a strongly nonohmic (Q-dependent) region which then saturates at a Q-independent value very close to T_λ [12–14]. Only the origin of this weak Q-independent singularity has been explained theoretically [15]. Although it is much more difficult to measure the thermal boundary resistance between normal fluid helium and the end plate, initial studies [15–17] suggest that a singular (and possibly Q-dependent) boundary resistance exists on this side of the transition as well. The depression of the superfluid transition temperature with a heat flux (mentioned above) was measured with the HeI–HeII interface forming at the bottom end plate of the cell [11]. Future measurements are planned to measure $T_\lambda(Q)$ when the interface reaches a sidewall platform, thus avoiding the end-plate effects. Since these end-plate effects (which fall off exponentially with the bulk correlation length ξ) become pronounced at much larger reduced temperatures than do the nonlinear bulk effects, they are often more than an order of magnitude larger than the predicted bulk nonlinear helium properties [9] we wish to study experimentally. Since we hope to make at least a 1% measurement of these bulk nonlinear properties, we must make our measurements at a distance at least 10ξ from either cell end plate. A reduced temperature $t=(T-T_\lambda)/T_\lambda=10^{-9}$ may be realistically

maintained in this experiment. At this reduced temperature, $\xi \approx 0.22$ mm, and the 10ξ rule would mandate that the measurements be made at least 2.2 mm from the end plates.

3. NEED FOR MICROGRAVITY

Experiments performed under gravity have qualitatively (yet not quantitatively) confirmed the existence of the nonlinear thermal conductivity region predicted by theory [19]. These measurements were made in small cells to avoid the convective onset. Hence, it appears to be very difficult to separate out conclusively the singular boundary effects from the nonlinear bulk thermal conductivity effects in these measurements. In these measurements only the helium very near the cold end plate of the cell was in the nonlinear region, while the remaining helium was in the linear region due to the thermal gradient across the helium layer. To observe other predictions from theory, such as the Q dependence of the interface width [and hence of $\xi(t=0)$], it is necessary to measure the actual thermal profile near and through the HeI–HeII interface with the highest possible thermal and spatial resolution. Only microgravity conditions sustained over many days will permit these effects to be conclusively studied experimentally.

One concern motivates the microgravity requirements for the static (heat capacity) experiments [5, 6], namely, the need to avoid the pressure-induced sample nonuniformity. For heat flux $Q \leqslant 0.1\ \mu\mathrm{W} \cdot \mathrm{cm}^{-2}$, this same concern applies to the dynamic measurements. At these small values of Q the pressure-induced variation in T_λ pushes the system away from criticality more than does the resulting thermal gradient in the normal fluid. At the opposite extreme, values of $Q > 3\ \mu\mathrm{W} \cdot \mathrm{cm}^{-2}$ create such a large thermal gradient in a 0.7-cm cell that they trigger the onset of convection in the normal fluid on Earth, thereby destroying our ability to measure the normal state's diverging diffusive thermal conductivity. Microgravity would permit much higher values of Q to be used [18]. Finally, the width of the HeI–HeII interface has been predicted to vary with $Q^{-1/2}$ [8, 9]. Under gravity, however, this cannot be directly measured since the gravitational field reduces the initial width of the $Q=0$ interface to only a few tens of micrometers. In orbit this initial $Q=0$ width has been predicted [8] to increase to about a millimeter, making its measurement thickness practical.

4. EXPERIMENTS

The measurements described above will be conducted within the experimental cell shown in Fig. 1. The sidewall platforms 3 and 2, located

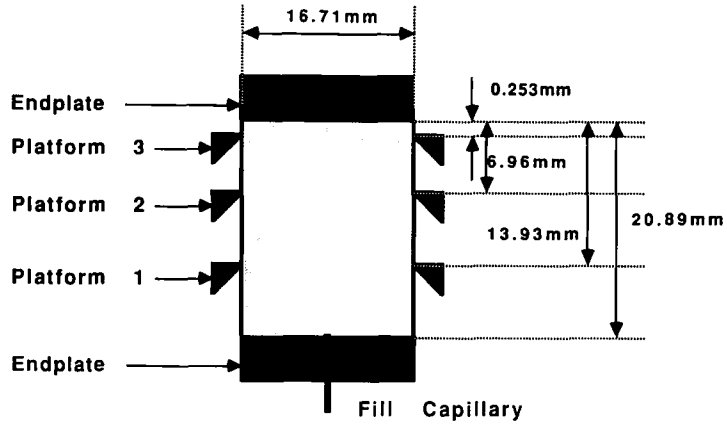

Fig. 1. The experimental cell constructed for these measurements. On Earth the cell is mounted with its fill capillary up. The heat fluxes from the bottom to the top to avoid convection (the isobaric thermal expansion coefficient is negative near T_λ). Both on Earth and in orbit the end plate with the capillary will be the cooler end of the cell.

253 μm and 7 mm from the warmer end plate, respectively, are used to measure the temperature profile as the interface is positioned at multiple locations very close to each ring. Measurements taken with platform 3 are affected by the nearby cell end plate near criticality, while measurements taken with platform 2 are not. Platform 1, located about 14 mm from the warmer boundary, is used to reference and control the superfluid phase temperature and to check for any thermal gradients in the superfluid at the higher values of Q. The interface is kept stationary until steady-state conditions are obtained.

The insulating sidewalls of the cell are constructed of aluminum alloy 5456 with a measured thermal conductivity of 0.020 $W \cdot cm^{-1} \cdot K^{-1}$ at 2.2 K. The isothermal cell end plates and the thermometry stages located along the cell's length are made of ultrapure (99.999 + %) aluminum which is expected to have a thermal conductivity of about 80 $W \cdot cm^{-1} \cdot K^{-1}$ [20]. This all-aluminum cell construction provides advantages over conventional cell designs. The cell is constructed by e-beam welded joints, making it robust to large accelerations and to repeated thermal cycling. In addition, this all-aluminum construction has only about one-third of the total cosmic ray absorption cross section per unit volume as that of a copper and steel cell construction, resulting in low parasitic heating from the cosmic flux once the apparatus is in orbit.

Each thermometry stage is constructed by machining two circular rings with a taper to produce a sharp edge on the inner diameter. Each ring

is thermally attached to its respective high-resolution thermometer through a 99.999 + % pure, 1-mm-diameter, aluminum wire which is threaded into a hole in the platform and welded in place. Following the e-beam weld of the platform ring to a groove machined into the sidewall, detailed optical studies and an electron microprobe analysis of the weld were performed, demonstrating excellent joining.

The pressure of the helium sample must be maintained to within about a millipascal to assure that pressure fluctuations do not create any more than a 0.1-nK fluctuation in T_λ. A vapor bubble may be used in a separate volume attached to the cell to maintain saturated vapor pressure conditions in the liquid. This vapor pressure bubble must be greater than 1 mm in radius to avoid pressure corrections from the liquid–vapor surface tension.

A very high thermal resolution near T_λ and exceptional spatial resolution at thermometry stages located along the sidewall of the cell are required to observe definitively the nonlinear thermal conductivity regime discussed above. Thermometers, similar in design to those developed at Stanford University within Prof. John Lipa's group [7], have been manufactured for this experiment by our group in collaboration with J.P.L. These thermometers differ from the Stanford design only in that they are fabricated from aluminum (rather than copper) for better cosmic ray immunity once in orbit. These thermometers, with noise levels approaching $0.2\,\mathrm{nK}\cdot\mathrm{Hz}^{-1/2}$ and close to the statistical limit of thermometry [21], provide adequate thermal resolution for this work. Variations on this thermometer design which use a toroidal geometry and simplified manufacturing procedures are currently under evaluation. The spatial resolution of the thermometry is greatly affected by the construction of the sidewall probe rings discussed above. The performance of these probe rings has been extensively modeled to optimize the design, as described below.

5. THERMAL SIMULATIONS

In all the thermal simulations discussed here the normal fluid helium bulk thermal conductivity λ is approximated [22] as $\lambda(t, Q) = [\lambda^{-4}(t, 0) + \lambda^{-4}(0, Q)]^{-1/4}$, where the zero-$Q$ thermal conductivity is approximated [16] as $\lambda(t, 0) = (122.2 + 7.05t^{-0.48})\,\mu\mathrm{W}\cdot\mathrm{cm}^{-1}\cdot\mathrm{K}^{-1}$ and the $t = 0$ limit of the thermal conductivity is taken as its theoretical value [9] as $\lambda(0, Q) = 27{,}400 \times Q^{-0.31}\,\mu\mathrm{W}\cdot\mathrm{cm}^{-1}\cdot\mathrm{K}^{-1}$, where Q is in units of $\mu\mathrm{W}\cdot\mathrm{cm}^{-2}$. In the equations above, the reduced temperature is defined relative to $T_\lambda(Q = 0)$. For $T < T_\lambda(Q = 0)$, the superfluid phase, the helium is forced isothermal by selecting $\lambda(\text{superfluid}) = 10{,}000\ \mathrm{W}\cdot\mathrm{cm}^{-1}\cdot\mathrm{K}^{-1}$. In these simulations the thermal conductivity of the aluminum alloy is taken

to be $0.01\ \mathrm{W \cdot cm^{-1} \cdot K^{-1}}$ and the conductivity of the 99.999+% pure aluminum is taken to be $100\ \mathrm{W \cdot cm^{-1} \cdot K^{-1}}$. The thermal boundary resistance R_k between all metal surfaces and the liquid helium is taken to be constant at $0.4\ \mathrm{cm^2 \cdot K \cdot W^{-1}}$. In these simulations the HeI–HeII interface is forced to remain at some height δ above the sidewall thermometry platform. The helium sample is isobaric.

A simulation of the thermal profile near the sidewall platform ring is displayed in Fig. 2. Here the HeI–HeII interface is located at $\delta = 50\ \mu\mathrm{m}$ above the platform ring and normal fluid exists at the position of the platform. A constant heat flux $Q = 0.1\ \mu\mathrm{W \cdot cm^{-2}}$ flows through the cell from the bottom to the top. Notice that the radial thermal gradient in the cell is large within about 1 mm from the sidewall. The temperature read by the

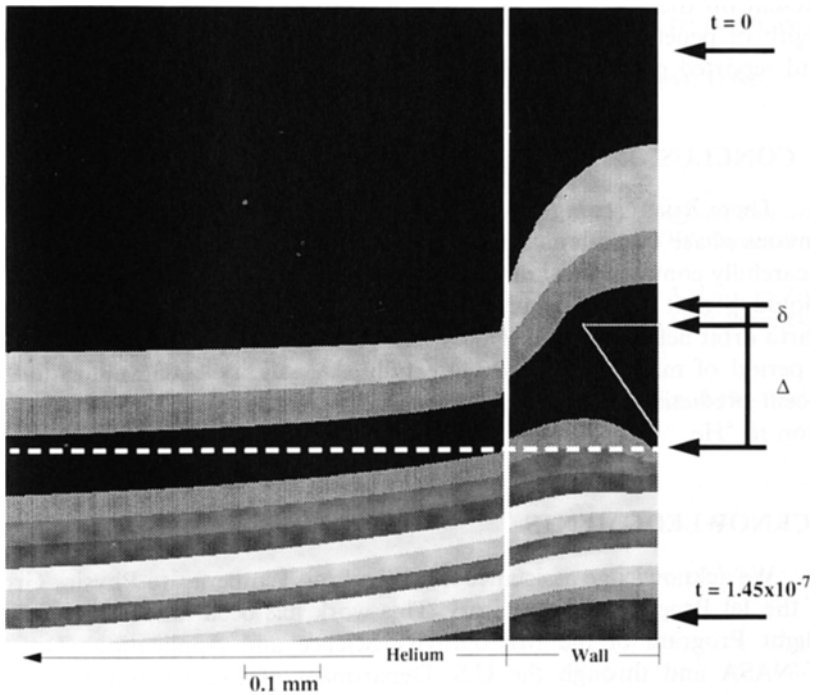

Fig. 2. Results of the thermal simulation for the thermal profile near the cell sidewall thermometry platform sampling the bulk helium. Here $Q = 0.1\ \mu\mathrm{W \cdot cm^{-2}}$ (flowing from bottom to top) and the HeI–HeII interface is located a distance $\delta = 0.05$ mm above the top of the platform. Each change in gray scale indicates a 10^{-8} change in the local reduced temperature t. The value of Δ is determined graphically by determining the height of the helium at the center of the cell which is isothermal with the platform (the dashed white line) and subtracting this height from the physical height of the platform. This Δ is nonzero only in regions where a radial component of the heat flux exists.

sidewall platform ring differs from the helium temperature near the center ($r = 0$) of the cell. The helium temperature near the center of the cell, where no radial temperature variation is noticed, is taken to be the true bulk helium temperature since it shows no sensitivity to the measurement apparatus at the sidewall (which is at $r = 8.35$ mm). Δ is determined graphically as displayed in Fig. 2. For a given Q, the variation of Δ on δ is weak and readily correctable, making the ultimate data analysis in this experiment tractable and not limited by these thermal offsets. Although virtually no heat is generated or absorbed in the thermometry platforms, the abrupt change in the sidewall's effective thermal conductivity in the vicinity of the platform creates a radial component of the heat flux which perturbs the otherwise purely axial heat flux through the cell. This radial heat flux integrated over the entire cell must equal zero since no sources/sinks are present on the platforms. The effect of the thermometry platform's shape, depth of penetration, and proximity to an end plate has been simulated and reported previously [23].

6. CONCLUSIONS

There exists strong scientific motivation to study the nature of continuous phase transitions in a system driven well away from equilibrium in a carefully controlled fashion. Technology is now under development which should permit such measurements at the superfluid transition in ^{4}He in Earth orbit before the year 2000. Microgravity conditions are required over a period of many days to explore fully the validity and ramifications of recent predictions for nonequilibrium effects through the superfluid transition in ^{4}He.

ACKNOWLEDGMENTS

We acknowledge assistance from the Low Temperature Physics Group of the Jet Propulsion Laboratory. This work has been funded through the Flight Program of the Microgravity Science and Applications Division of NASA and through the U.S. Department of Energy under Contract DE-AC04-76DP00789.

REFERENCES

1. Available from Helium Operations, Bureau of Mines, Department of the Interior, 801South Fillore, 500, Amarillo, TX, 79101-3545.
2. P. C. Hendry and P. V. E. McClintock, *Cryogenics* **25**:526 (1985).

3. V. L. Ginzburg and A. A. Sobyanin, *J. Low Temp. Phys.* **49**:507 (1982).
4. G. Ahlers, *Phys. Rev.* **171**:275 (1968).
5. Lambda Point Experiment, Principal Investigator, J. Lipa, Stanford University, Palo Alto, CA.
6. Confined Helium Experiment, Principal Investigator, J. Lipa, Stanford University, Palo Alto, CA.
7. J. A. Lipa, B. Leslie, and T. Wallstrom, *Physica* **107B**:331 (1981).
8. A. Onuki, *J. Low Temp. Phys.* **50**:433 (1983), **55**:309 (1934), and references therein.
9. R. Haussmann and V. Dohm, *Phys. Rev. Lett.* **67**:3404 (1991); *Z. Phys.* **B87**:229 (1992).
10. R. Haussmann and V. Dohm, *Phys. Rev. B* **46**:6361 (1992).
11. R. Duncan, G. Ahlers, and V. Steinberg, *Phys. Rev. Lett.* **60**:1522 (1988).
12. R. Duncan, G. Ahlers, and V. Steinberg, *Phys. Rev. Lett.* **58**:337 (1987); R. Duncan and G. Ahlers, *Jpn. J. Appl. Phys. (Suppl.)* **26**(3):363 (1987); *Phys. Rev. B* **43**:7707 (1991).
13. M. Dingus, F. Zhong, and H. Meyer, *J. Low Temp. Phys.* **65**:185 (1986); F. Zhong, J. Tuttle, and H. Meyer, *J. Low Temp. Phys.* **79**:9 (1990); D. Murphy and H. Meyer, unpublished.
14. T. C. P. Chui, Q. Li, and J. A. Lipa, *Jpn. J. Appl. Phys. (Suppl.)* **26**(3):371 (1987); Q. Li, T. C. P. Chui, and J. A. Lipa, *Bull. Am. Phys. Soc.* **33**:1373 (1988).
15. D. Frank and V. Dohm, *Phys. Rev. Lett.* **62**:1864 (1989); *Z. Phys.* **B84**:443 (1991).
16. G. Ahlers and R. V. Duncan, *Phys. Rev. Lett.* **61**:846 (1988).
17. Q. Li, Ph.D. thesis (Stanford University, Palo Alto, CA, 1990).
18. R. P. Behringer, *Rev. Mod. Phys.* **57**:657 (1985).
19. F.-C. Liu and G. Ahlers, *Physica B* **194–196**:597 (1994); unpublished.
20. Y. S. Touloukian, R. W. Powell, C. Y. Ho, and P. G. Klemens, *Thermophysical Properties of Matter, Vol. 1. Thermal Conductivity: Metallic Elements and Alloys* (IFI/Plenum, New York, 1970).
21. T. C. P. Chui, D. R. Swanson, M. J. Adriaans, J. A. Nissen, and J. A. Lipa, in *Temperature: Its Measurement and Control in Science and Industry, Vol. 6* (AIP Press, New York, 1992), pp. 1213–1218.
22. F.-C. Liu and G. Ahlers, unpublished.
23. R. Duncan, R. Akau, S. Gianoulakis, U. Israelsson, and T. Chui, *Physica B* **194–196**:603 (1994); unpublished.